Fabrication of a Fresnel zone plate through electron beam lithographic process and its application to measuring of critical dimension scanning electron microscope performance

J. Kim[a] and K. Jalhadi
Electron Beam Laboratory, University of Tennessee, Knoxville, Tennessee 37996-0840

S.-Y. Lee
Department of Electrical and Computer Engineering, Auburn University, Auburn, Alabama 36849

D. C. Joy
Electron Beam Laboratory, University of Tennessee, Knoxville, Tennessee 37996-0840
and Oak Ridge National Laboratory, Oak Ridge, Tennessee 37831

(Received 21 March 2007; accepted 28 August 2007; published 12 October 2007)

It is important to be able to quantify the imaging performance of critical dimension scanning electron microscopes for such purposes as verifying the specification, and tracking and optimizing its performance during use. Imaging performance can be defined by parameters such as resolution, signal to noise ratio, drift, and instability under standard operation conditions. To perform tests to obtain such parameters, it is necessary to have both suitable test samples and appropriate software for image analysis. A Fresnel zone plate, as a reproducible and well characterized sample, is fabricated using direct-write electron beam lithography. A package of two-dimensional Fourier transform and analysis software, designed as a plug-in for the shareware IMAGE-JAVA program, has been developed for resolution analysis and is freely available online. © *2007 American Vacuum Society.* [DOI: 10.1116/1.2787874]

I. INTRODUCTION

As semiconductor device dimensions continue to shrink, methods to determine precisely and correctly the size of a given structure become an important issue because the physical dimensions have a direct impact on chip performance. In the early days, linewidths were large enough to be imaged and measured on optical microscopes, but current device design rules result in structures which are so small as to challenge the performance of even the best scanning electron microscopes (SEMs) by being required to routinely achieve a spatial resolution below 1.0 nm.

In order to obtain the optimum performance from a scanning electron microscope, it is necessary to be able to characterize and quantify its performance reliably and rapidly and compare the imaging parameters of one tool with those of others, in terms of resolution, signal to noise ratio, drift, and instability under standard operating conditions. An essential requirement for making such measurements is a specimen which contains features sufficiently small to test the resolving power of the instrument. The sample should also be stable under the electron beam and should neither charge nor contaminate during imaging and ideally it should consist of multiple, identical copies of the same target area so that repeat measurements can be made or so that different microscopes can be tested by reference to the same specimen.

This article describes the construction of a suitable test imaging artifact consisting of an array of Fresnel zone plate (FZP) pattern with an outer diameter of about 2 μm and a minimum feature size of about 20 nm and the results obtained by an image analysis program using the FZP as a sample. The Fresnel structure was chosen for this purpose because it has already been widely used for the characterization of optical imaging systems since it generates a wide and relatively flat Fourier spectrum and because its circular symmetry tests the X and Y linearities of the imaging scan and facilitates the optimization of astigmatism correction. The Fresnel structures are fabricated by electron beam lithography processes onto standard silicon wafers, rather than onto thin substrates, in order to make them suitable for use in critical dimension scanning electron microscope (CD-SEM) systems and to ensure their mechanical integrity even though this increases the practical problems of the fabrication process. By using electron beam lithography, it is possible to make a large number of identical copies of the structure on the wafer and to repeat the process for as many wafers as might be required. In this way, repeat measurement and comparative measurement on different machines or at different locations can all be performed on what are effectively identical specimens.

II. BASIC TECHNIQUES

The procedures employed here to determine the imaging resolution and to extract additional information about the parameters which describe the imaging performance are based on the use of two-dimensional power spectra (diffractograms) obtained from the Fourier analysis of recorded SEM images. These methods are commonly used for the

[a]Electronic mail: jkim7@utk.edu

analysis of optical tools and provide a consistent and thorough way of quantifying many aspects of the imaging behavior. The program now in use is a development from the SMART routine described earlier,[1,2] which was a macroroutine in the public domain designed to work with the widely disseminated public domain image analysis programs NIH IMAGE (Ref. 3) and SCION IMAGE.[4] When installed in IMAGE, the SMART macro provides the automated routines which measure the spatial information transfer limit (i.e., resolution) and the accuracy of image stigmation, can determine resolution and tool stability from a pair of sequentially recorded images (superposition diffractograms), and determines the signal to noise ratio of digitally stored images for such purposes as measuring the electron detector quantum efficiencies.[5] In this version, the SMART package has been widely used and has proven to be a valuable diagnostic tool for the setting up and routine testing of electron beam tools.

However, upgrades and enhancements for both the original Macintosh-based NIH IMAGE and the later Windows-based SCION IMAGE programs have now ceased and both variants have been replaced by IMAGE JAVA,[6] which replicates most of the facilities of the original programs but, recorded in JAVA, is now platform independent and therefore more widely applicable. To accommodate this change, the original SMART macro, which was written in a Pascal-like language, had to be replaced by a new SMART-J plug-in written in C++ which properly interfaces with the tools provided by IMAGE-J. The facilities provided by IMAGE-J, and as further extended by SMART-J, are similar to those of the original Mac or Windows versions although offering more facilities but a little less convenience because of some of the restrictions imposed by the use of JAVA. The full source code and documentation for the SMART-J plug-in, ready to be compiled and incorporated into IMAGE-J, are available from our website (http://pciserver.bio.utk.edu/metrology) or directly from the authors. Specifically, SMART-J can produce and analyze single image diffractograms to measure the spatial resolution and accuracy of stigmation correction; it can generate superposition diffractograms from a sequential pair of images to more precisely determine resolution and measure tool drift and instability, and it can measure the signal to noise ratio of stored digital images. Further enhancements provide the ability to obtain the optical transfer function of the tool from an image,[7] and generate data on quantities such as image entropy and normalized measures of performance[8] although these options are not covered in this article.

III. TARGETS FOR TOOL TESTING

The factor which has most limited the application of Fourier and other rigorous analytical techniques to measuring the imaging performance of tools has been the availability of suitable test targets. The common practice has been to use specimens such as gold or platinum particles dispersed on a carbon substrate for the determination of imaging resolution because they can be easily prepared and provide high contrast and a useful amount of high spatial frequency information. However, these samples, each of which is unique, are random, poorly controlled, and irreproducible. Such samples also typically contain materials which could introduce contamination if used inside *inline* tools. Consequently, when using such samples it is impossible to generate reliable results, either to properly verify a specification or to compare two tools in different locations. The ideal sample would be the one that can be replicated at a low cost with the same specification and offers high-contrast, isotropically dispersed detail with spatial frequency components which extend beyond the resolution range of the imaging tool. With such a specimen, the Fourier transform power spectrum would be limited only by the imaging performance of the tool rather than being constrained by the sample.

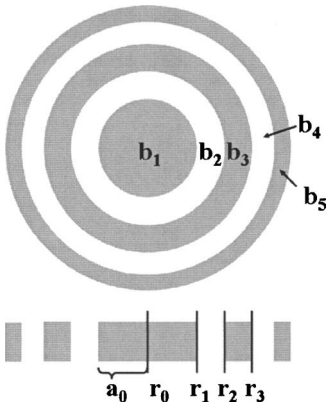

FIG. 1. Schematic description of constructing a Fresnel zone plate.

A. Choice of target design

The chosen target structure is a Fresnel zone plate which in this version consists of concentric rings where the radius r_n of the nth ring (r_0 corresponds to the center of a zone plate) is calculated by the equation of $r_n = a_0\sqrt{n}$ and the areas b_n and b_{n+1} are identical (refer to Fig. 1). A FZP is a highly dense and symmetric structure, and can be fabricated on the nanoscale so that, depending on the number of rings and their widths and diameters, such a zone plate provides a wide and flat Fourier spectrum. The effective limit for determining resolution with the zone plate depends on the largest ring diameter since this defines the field of view required to record the complete image. Thus, for a FZP 2.0 μm in diameter, a field of view just able to fully accommodate the structure and 1000 pixels in width would give a pixel size of 2 nm and a Fourier limit of 4 nm (i.e., 2 pixels in size). To obtain resolution data at higher resolutions will require either features with a smaller overall diameter or the collection of images containing a higher number of pixels. The FZP is fabricated through the electron beam lithographic process, and thus can be replicated in as many identical copies as required, once the fabrication conditions are optimized.

B. Fabrication of Fresnel zone plates on Si substrate

The target FZP consists of 13 concentric rings, with the diameter of the outermost ring being 2.08 μm and the mini-

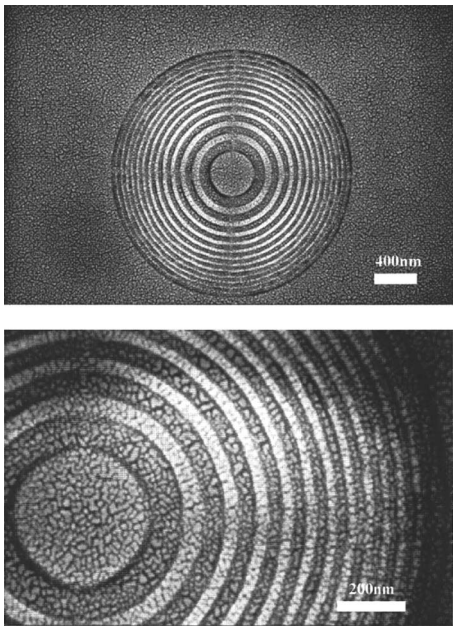

FIG. 2. Fresnel zone plate fabricated on 50 nm PMMA with the base dose of 160 $\mu C/cm^2$.

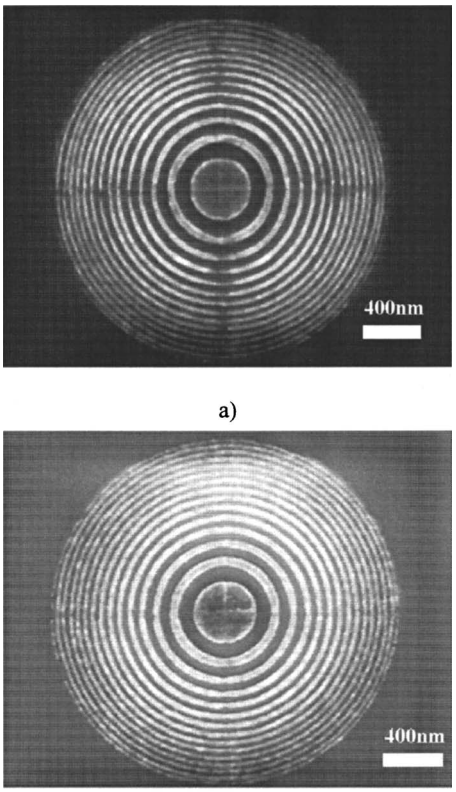

FIG. 3. Fresnel zone plate fabricated on 50 nm HSQ: (a) the base dose of 480 $\mu C/cm^2$ and developed in 0.26 N tetramethylammonium hydroxide (TMAH) for 70 s, TMAH: deionized water (D.I.W)=1:9 for 10 s and D.I.W for 10 s and (b) the base dose of 460 $\mu C/cm^2$ and developed in 0.26 N TMAH for 70 s, TMAH: D.I.W=1:10 for 60 s, and D.I.W for 60 s. SEM images are taken at 2 keV on a LEO 1525 scanning electron microscope.

mum ring width of 20 nm. Initially, the pattern was transferred onto 50 nm polymethylmethacrylate (PMMA) spun onto Si wafers with a direct-write electron beam lithographic process. FZP structures which are to be used as lenses for x-ray or high energy ultraviolet light are fabricated onto thin transparent substrates such as silicon nitride and as a result there is little need for proximity effect correction because both beam spreading and backscattering are minimal. However, in our application, the Fresnel zone plate structures are designed to be used in CD-SEMs or other electron beam tools which work exclusively with wafers. A consequence of the wafer substrate is that proximity effect corrections become significant and essential.

In order to achieve the necessary correction for proximity effects, the FZP pattern was analyzed by a version of PYRAMID designed specifically for nonrectangular features.[9] This algorithm computes the pixel by pixel electron beam dose so that the final exposure (energy deposited) is as uniform as possible over all rings. Typical SEM images of a FZP fabricated as discussed are shown in Fig. 2. The size, symmetry, and ring spacing of the desired pattern have generally been transferred with high fidelity demonstrating the success of the proximity effect corrections. Absolute pattern size (e.g., linewidth and spacing) is not of first importance for the described application of evaluating CD-SEM optical performance.

Although FZP patterns were successfully fabricated using PMMA resist, as described above the resultant resist structure does not provide high contrast for secondary electron imaging in the SEM without metal coating such as chromium, tungsten, or iridium. Because a high contrast is desirable to maximize the signal to noise ratio of the image, a similar FZP pattern was fabricated using hydrogen silsesquioxane (HSQ) as the resist. In this case, the final structure after development is essentially amorphous silicon oxide which charges lightly under the beam and gives good imaging contrast, and it is also compatible with tools to be used inline. In this version (see Fig. 3), the pattern consists of 15 rings, where the diameter and width of the outermost ring are 2.1 μm and 18 nm, respectively. Although the HSQ patterns are less geometrically precise than those made in PMMA which would not be ideal for a FZP designed for use as a focusing option, it is of no consequence for the purpose of measuring tool imaging performance. For this application, the only parameters that are important are the radial symmetry and the harmonic relationship between the radii of the rings since it is these quantities which provide the desired spatial power spectrum for analysis. The FZP structure fabricated with HSQ provides a usefully enhanced level of imaging contrast as compared to the PMMA version when observed in the secondary electron mode of a SEM at the beam energy over the range of 500 eV to 2 keV.

IV. APPLICATION OF ANALYSIS PROGRAM

A nanofabricated HSQ Fresnel zone plate and the SMART-J/IMAGE-J software can be used to determine the im-

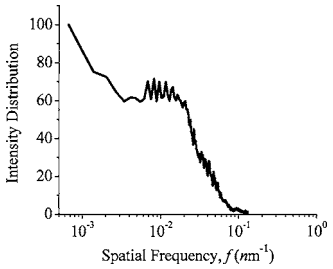

FIG. 4. Intensity distribution normalized by the maximum value is plotted as a function of spatial frequency f.

aging resolution of the tool under the chosen imaging conditions. The basis of the method is to obtain a diffractogram in the form of a power spectrum, i.e., the two-dimensional Fourier transform, displayed as an intensity plot.[10] As a first step, the FZP is imaged at the highest magnification which permits the complete zone plate structure to be captured, as shown in Fig. 3. This guarantees the minimum possible pixel size. The IMAGE-J/SMART-J program displays the image contents by plotting the intensity distribution as a function of spatial frequency, as shown in Fig. 4. The signal intensity decreases with increasing frequency (i.e., going away from the center of the diffractogram) and finally drops to the level of random background noise. The diffractogram power spectrum computed through the fast Fourier transform can be quantified in one of the two ways. The "automatic mode" fits an ellipse around the threshold region which represents the signal information, as illustrated in Fig. 5. The major and minor axes of the ellipse (in units of inverse nanometers) are recorded to yield an overall resolution value in nanometers. The eccentricity E of the ellipse, i.e., the deviation from the ideally isotropic pattern, is defined as the following equation:

$$E = \frac{(L_{\mathrm{maj}} - L_{\mathrm{min}})}{L_{\mathrm{maj}}},$$

where L_{maj} and L_{min} are the lengths of the major and minor axes, respectively. The eccentricity measures the stigmatic error which should be less than 0.1 and ideally less than 0.05 in a well aligned and operated tool. The "manual mode" superimposes concentric circles, representing the spatial

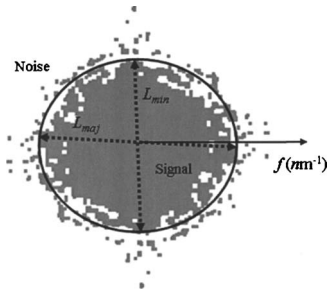

FIG. 5. Diffractogram power spectrum of the central 512×512 pixel region of the image shown in Fig. 3. The power spectrum is thresholded to show the boundary between signal and noise, which defines the spatial resolution. Spatial frequency f increases as going away from the center of power spectrum.

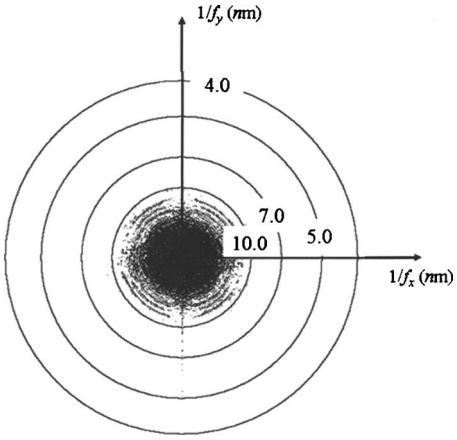

FIG. 6. Manual mode analysis of the power spectrum derived from the image shown in Fig. 3. The superimposed circles are calibrated directly in units of nanometers. The f_x and f_y represent spatial frequencies in the x and y directions, respectively, where $f = \sqrt{f_x^2 + f_y^2}$.

resolution in nanometers, over the power spectrum display which is directly calibrated, as shown in Fig. 6. The concentric circle corresponding to the outer boundary of diffractogram represents the resolution of the image and the stigmatic correction is judged visually. In either mode, the highest spatial resolution obtained from the power spectrum is limited to the interval of 2 pixels, and thus images must be taken at a sufficiently high magnification to have the pixel size at least a factor of 3 smaller than the anticipated resolution limit of the tool. We obtain the spatial resolution of about 13–15 nm and eccentricity of 0.13 calculated and judged from obtained spectra.

Although the above approach can provide reliable data on resolution and the accuracy of stigmatic correction, it is subject to two significant deficits. Separating the signal from noise on the power spectrum is performed by manually setting the threshold, although the boundary between the signal and noise from a single image cannot be determined on a pixel by pixel basis. Therefore, there is a certain degree of uncertainty in defining the resolution properly even for a skilled operator. The second limitation is that the resolution obtained from a single image only represents the tool performance over the relatively short period used for the image recording. Time-dependent parameters such as beam drifting, focus variation, and power supply instabilities can degrade the repeatability of parameters and precision of the tool and thus affect the overall performance of the tool.

Thus, these limitations can be overcome by applying the "superposition diffractogram mode" that is also offered by SMART-J.[11] In this mode, two sequential images taken a few minutes apart and under identical imaging conditions are digitally superimposed with a horizontal offset of typically 16 or 32 pixels to form a composite micrograph. The diffractogram of this composite looks like the power spectrum of either image but is crossed by a fringe pattern whose spacing is inversely proportional to the offset imposed. This method, first described by Frank *et al.*,[11] has been widely used for measuring the performance of transmission electron micro-

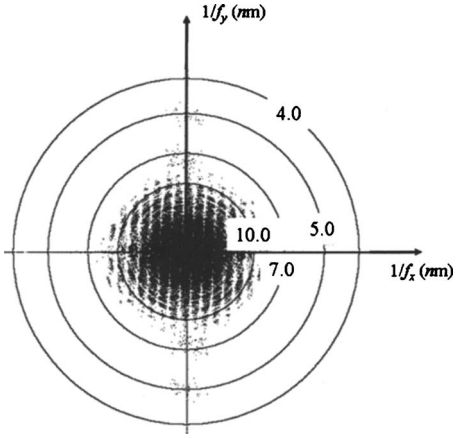

FIG. 7. Power spectrum obtained from superposition diffractogram mode.

scopes but is also applicable to the SEMs.[10] The fringes crossing the power spectrum represent interference ("Youngs fringes") between details present in both versions of the images, and the power ratio of the coherent signal fringes to the incoherent noise is enhanced by a factor of 4. The fringes vanish at the spatial frequency at which the signal vanishes into the noise. There is thus no uncertainty in identifying the maximum spatial frequency of information transfer in the images. Figure 7 shows a superposition diffractogram generated from the FZP. The two images analyzed were recorded at 2 keV in a LEO field emission gun SEM at a magnification of 31000× and taken with a 40 s time interval between exposures. The measured resolution is about 10–12 nm which is a slightly more optimistic estimate when compared to the resolution of 13–15 nm obtained from the single image procedures. This is because the high fringe modulation contrast (signal) is now easily distinguished from the weak, unmodulated, noise background. The information on the precision and stability of tool over the time interval required to record the two images is also obtained through the analysis of the superposition diffractogram. The fringes in the diffractogram are due to the lateral offset between the two images, and should therefore be completely vertical. Any deviation from the vertical indicates that there has been some type of beam or stage drifting or instability. The magnitude of the drift over the elapsed time period D can be expressed by the following relationship:

$$D = 2[(\text{pixel offset})\ \text{pixel size (nm)}]\sin(\theta/2),$$

where θ is the angle between the fringe pattern and the vertical. Here, the pixel offset is 32 pixels with the pixel size of 3.8 nm, and θ is 3.5°, so the drift D is 7.43 nm over a period of 40 s. Consequently, the drift rate less than 1 nm/s is readily identified and measured by this method.

V. SUMMARY

A Fresnel zone plate is successfully fabricated on PMMA and HSQ resists using the electron beam lithographic process and the proximity correction program (PYRAMID) for optimizing imaging targets. Especially the zone plate structure fabricated on HSQ resist provides a useful level of imaging contrast and the symmetric structure which make it possible to achieve optimum imaging performance. The combination of the software package designed to provide diffractogram through the fast Fourier transform and the fabricated Fresnel zone plate provides the ability to quickly and accurately measure the imaging resolution of a SEM. In particular, the superposition diffractogram method employing two sequential images which are taken with a realistic time interval is a highly useful method for determining the resolution of a tool because of the enhanced true information through the correlation between the two images. The ability to replicate the same specification of measurement samples through the electron beam lithographic process makes it possible to compare the performance of instruments in different locations and collect the performance data from a given instrument over time.

ACKNOWLEDGMENTS

The authors are grateful to J. A. Liddel (LBNL) for valuable discussions on Fresnel zone plate fabrication, and the Brendan Griffin (University of Western Australia) and G. Lorusso (KLA-Tencor) for their testing and significant contributions to the SMART routines.

[1] D. C. Joy, Y.-U. Ko, and J. J. Hwu, Proc. SPIE **3998**, 108 (2000).
[2] D. C. Joy, J. Microsc. **208**, 24 (2002).
[3] NIH IMAGE can be downloaded from http://rsb.info.nih/nih-image
[4] SCION IMAGE is an authorized port of NIH IMAGE for Windows and can be downloaded from http://www.scioncorp.com
[5] D. C. Joy, C. S. Joy, and R. D. Bunn, Scanning **18**, 533 (1996).
[6] IMAGE JAVA can be downloaded from http://rsb.info.nih.gov/ij
[7] A. Mauly and G. L. Farrent, Proc. SPIE **3998**, 108 (2000).
[8] M. Sato and J. Orloff, Ultramicroscopy **41**, 181 (1992).
[9] S.-Y. Lee, F. Hu, and J. Ji, J. Vac. Sci. Technol. B **22**, 2929 (2004).
[10] S. J. Erasmus, D. M. Holburn, and K. C. A. Smith, Inst. Phys. Conf. Ser. **52**, 73 (1980); see also A. E. Vladar, M. T. Postek, and M. P. Davidson, Scanning **20**, 24 (1997).
[11] J. Frank, P. Bussler, R. Langer, and W. Hoppe, Ber. Bunsenges. Phys. Chem. **74**, 1105 (1970). See also Ref. 10 for the earliest application of the technique to SEM imaging.